Supporting Information

Impact of DNA-Surface Interactions on the Stability of DNA Hybrids

Sarah M. Schreiner,[†] Anna L. Hatch,[†] David F. Shudy,[†] David R. Howard,[‡] Caitlin Howell,[§,∥] Jianli Zhao,[∥] Patrick Koelsch,[§,∥] Michael Zharnikov,[∥] Dmitri Y. Petrovykh,*[,⊥] Aric Opdahl*[,†]

[†]*Department of Chemistry, University of Wisconsin—La Crosse, La Crosse, WI 54601, USA;* [‡]*Department of Biology, University of Wisconsin—La Crosse, La Crosse, WI 54601, USA;* [§]*Institute of Toxicology and Genetics, Karlsruhe Institute of Technology, Hermann-von-Helmholtz-Platz 1, 76344 Eggenstein-Leopoldshafen, Germany;* [∥]*Angewandte Physikalische Chemie, Universität Heidelberg, Im Neuenheimer Feld 253, 69120 Heidelberg, Germany;* [⊥]*Department of Physics, University of Maryland, College Park, MD 20742, USA*

**E-mail: opdahl.aric@uwlax.edu, dpetrovykh@inl.int*

MATERIALS AND METHODS

Materials. Custom oligonucleotides, purchased from commercial DNA vendors, are written here in the 5' to 3' direction. Sequences used in hybridization experiments included a 15-nucleotide adenine homo-oligo (A15); a 15-nucleotide thymine homo-oligo (T15); a mixed sequence of 15 nucleotides (5'-CAATGCAGATACACT-3', denoted P15) and its full complement (5'-AGTGTATCTGCATTG-3', denoted P15'). These sequences were incorporated as components (blocks) into longer self-complementary DNA strands, including A15–T20; P15–T5–P15'; and P15'–A5–P15. Oligos denoted with –SH have a 3' thiol modification and were used in the as-received asymmetric disulfide form, i.e., without removing the –S–$(CH_2)_3$–OH protecting group from the 3' end (Refs 8, 21). The sequence denoted A15–T30* is labeled with fluorescent TAMRA at the 3' end. Buffers denoted NaCl-TE and $CaCl_2$-TE contained 1 M NaCl or $CaCl_2$, respectively, 1×TE (10 mM Tris·HCl, 1 mM EDTA), and were adjusted to pH 7 with HCl. The 1-mercapto-6-hexanol (MCH) was purchased from Fisher Scientific. The 1-mercapto-11-undecyl triethylene glycol (PEG–SH), was obtained from Asemblon (Redmond, WA).

Gold Substrates. Commercial SPR glass slides coated with ca. 47 nm of gold were used for SPR analysis. Substrates for XPS and NESAFS analysis were Si(100) wafers coated with 5 nm of Ti followed by 100 nm of Au. Gold surfaces for SPR, XPS, and confocal microscopy experiments were cleaned with piranha solution [70% H_2SO_4 30% H_2O_2 (30% H_2O_2 in H_2O)] and rinsed thoroughly with deionized water (18.2 MΩ) immediately prior to use. *Caution*: Piranha solution is extremely oxidizing, reacts violently with organics, and should be stored in loosely covered containers to avoid pressure buildup.

DNA Immobilization. For probes without thiol modifications, DNA immobilization followed a standard procedure that yields high surface densities (Refs 11, 15): clean gold surfaces were incubated at 35 °C for 20 h with DNA solutions (4 μM DNA in $CaCl_2$-TE buffer). After immobilization, each sample was rinsed sequentially with deionized water, NaCl-TE buffer, 0.1 M NaOH, and deionized water, before drying under flowing nitrogen. This four-step rinse procedure removes calcium ions and weakly bound DNA from the surface. For probes with thiol functionality, immobilization from 4 μM DNA solutions in NaCl-TE buffer for ca. 2 h at room temperature was used to produce probe surface densities comparable to those of unmodified probe sequences. Hybridization solutions contained 4 μM target DNA in NaCl-TE buffer at room temperature.

Patterned Samples for Fluorescence Measurements. Simple DNA arrays with 500×500 μm^2 square gold regions surrounded by a monolayer of PEG–SH were prepared by soaking piranha-cleaned SPR sensors for 20 h in ethanolic 1 mM PEG–SH (Asemblon, Redmond, WA), rinsing, drying, covering with a mask, and treating for 2 h under a 500 W UV mercury arc lamp equipped with a liquid IR filter. This exposure produced an array of 500×500 μm^2 squares of UV-cleaned gold separated by PEG–SH regions. The patterned SPR sensors were rinsed with ethanol and buffer solution prior to DNA probe immobilization. Fluorescent A15–T30* probes were then immobilized in the clean gold regions following the procedure described above.

Samples for NEXAFS Measurements. Gold surfaces for NEXAFS experiments were cleaned for 2.5 h in a commercial UV/ozone cleaner. A5–T15, A15, and T6–SH probes were immobilized on clean gold substrates at 37 °C for 40 h from 3 μM DNA solutions in $CaCl_2$-TE buffer. Samples were then washed under flowing deionized water for ca. 1 min and dried under flowing nitrogen. Some of the freshly rinsed A5–T15 samples were immersed into a 3 μM solution of A15 targets in NaCl-TE buffer for 8 h at room temperature. Samples were then rinsed under flowing NaCl-TE buffer for ca. 1 min, *briefly dipped* into deionized water to remove excess salts, and dried under flowing nitrogen. The samples were stored under inert gas atmosphere in glass containers until they were transferred into vacuum for measurements at the synchrotron radiation facility.

Surface Plasmon Resonance (SPR). DNA immobilization and hybridization were measured *in situ* using an SPR imaging system (GWC, Madison, WI) as described previously (Ref 15). Our quantitative analysis followed established methods outlined by Jung *et al*. (Refs 15, 23). We assumed the effective "bulk" values of DNA density (1.7 g/cm^3) and refractive index (1.7) that are commonly used as parameters for SPR quantification (Ref 15).

To obtain quantitative measurements during the stringency rinse experiments (Ref 15), SPR sensors prehybridized in 1 M NaCl were rinsed with successively lower ionic strength buffer solutions for 4 min. After each rinse step, a blank 1 M NaCl buffer was flowed through the liquid cell and the change in reflected light was recorded. Returning to the original 1 M NaCl buffer solution after each step produces measured changes in light intensity that can be directly attributed to DNA loss, thus eliminating the need to account for differences in refractive indexes of the rinse buffers (Ref 15).

X-ray Photoelectron Spectroscopy (XPS). Quantitative XPS analysis was used to measure surface densities of DNA probes *ex situ* for several witness samples, which were prepared similarly to samples used in SPR and NEXAFS measurements. XPS was performed in a system equipped with a monochromatic Al Kα source, a magnetic electron lens, and a hemispherical electron energy analyzer; data were analyzed using methods previously described in Refs 11 and 21.

Fluorescence Microscopy. Laser-scanning confocal fluorescence microscopy images were obtained using a Nikon CS1 confocal system. Images were obtained using a 40× oil 1.3 NA objective, 561 nm diode pumped solid state laser, and PMT detection. A simple liquid cell was constructed using double-sided tape to form a channel between the gold coated slide and a

glass coverslip (Ref 24). Image brightness and contrast were adjusted for clarity of presentation.

NEXAFS. Near-edge x-ray absorption fine structure (NEXAFS) spectroscopy measurements were made on beamline D1011 at the MAX II storage ring at the MAX-lab synchrotron radiation facility in Lund, Sweden. The spectra at the nitrogen K-edge were acquired under linearly polarized light (ca. 95% polarization) in the partial electron yield mode with retarding voltage of -300 V. The energy resolution was <100 meV; the energy scale was referenced to the most intense π* resonance of highly oriented pyrolytic graphite at 285.38 eV (Ref 25). The incidence angle of the x-rays was varied from 90° (**E**-vector in the surface plane) to 20° in steps of 10°–20° to monitor the orientation and ordering of nucleobases within the DNA films.

The raw NEXAFS spectra were normalized to the incident photon flux by division through a spectrum of a clean, freshly sputtered gold sample. The spectra then were reduced to the standard form by subtracting linear pre-edge background and normalizing to the unity edge jump (determined by a nearly horizontal plateau 40–50 eV above the absorption edge).

RESULTS

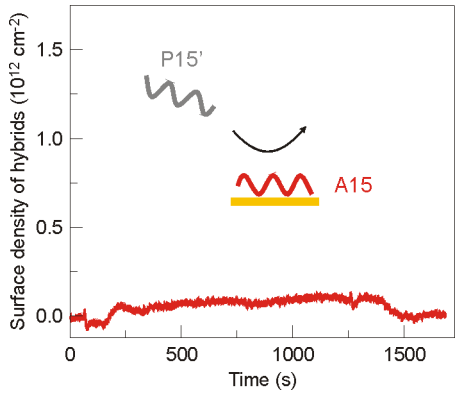

Figure S1. Typical SPR signal for an attempted hybridization of non-complementary target with A15 probes immobilized on gold. A clean SPR sensor was pre-incubated to produce saturation surface density of ca. 1.3×10^{13} cm^{-2} of unmodified A15 probes on gold (data for A15 immobilization not shown), then exposed for ca. 20 min to 4 μM solution of a P15' target in 1 M NaCl-TE buffer, followed by a rinse for ca. 5 min in blank buffer. Note that the signal returned to baseline after the buffer rinse, indicating no significant hybridization. Diagram depicts idealized representations of P15' targets (gray) and A15 probes (red). The target sequence denoted P15' was the same as in Figure S2.

Hybrids of Mixed-Composition Sequences. We test the generality of the trends observed for A:T hybrids by performing experiments parallel to those in Figures 1 and 2 for hybrids formed by complementary P15 and P15′ sequences that have mixed nucleotide compositions. In contrast to the A:T models, in which the high affinity of (dA) blocks for gold unambiguously defined the component of a hybrid that was strongly interacting with the surface, no such *a priori* asymmetry can be expected between P15 and P15′ sequences. Nevertheless, gold surfaces functionalized with unmodified P15 and P15–T5–SH probes behave in hybridization experiments with P15′ targets (Figure S2a) in a manner similar to the directly-adsorbed A15 and end-tethered T15–SH probes, respectively, in Figure 1a. Furthermore, the stability of the resulting P15′:P15 and P15′:P15–T5–SH hybrids (Figure S2b) qualitatively follows the trends of the directly-adsorbed and end-tethered hybrids in Figure 1b, indicating that the range of properties expected for P15′:P15 hybrids in different conformations is comparable to that observed for the model A:T hybrids in Figures 1 and 2.

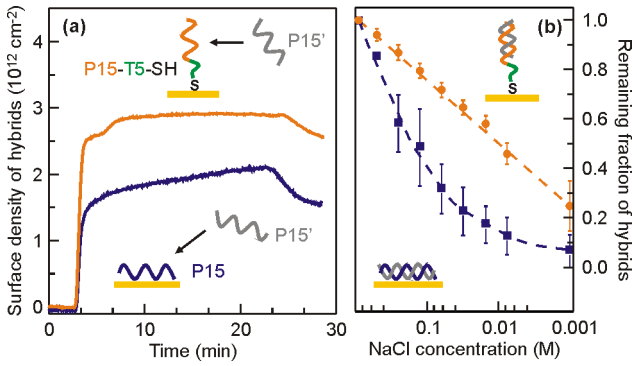

Figure S2. Formation and stability of hybrids formed with mixed-composition probes in directly-adsorbed and end-tethered conformations. Diagrams depict idealized representations of each target–probe pair (orange = P15–T5–SH and blue = P15 probes; gray = P15' target) before and after hybridization (a) and during melting (b). The line and symbol colors in the data plots correspond to the color-coding of the respective probes: end-tethered P15–T5–SH (orange) or directly-adsorbed P15 (blue). In each hybridization experiment (a), the sensor was exposed for ca. 20 min to 4 μM solution of a target in 1 M NaCl-TE buffer, followed by a rinse for ca. 5 min in blank buffer to remove any weakly bound DNA targets. The stringency rinse profiles in (b) were obtained by exposing *prehybridized* SPR sensors to solutions of successively lower NaCl concentration and monitoring the number of hybrids remaining on the surface. The probe sequence denoted P15 was 5'-CAATGCAGATACACT-3'; complementary target denoted P15' was 5'-AGTGTATCTGCATTG-3'. Error bars in panel (b) represent variation among replicate samples.

Relative Stabilities of Double-Stranded P15′:P15 Hybrids. The trends between relative stabilities of directly-adsorbed and end-tethered P15′:P15 hybrids in competitive experiments parallel those observed in Figure 2 for the A:T hybrids. The comparison between the two conformations in Figure S3 is more direct than that in Figure 2 because a comparable density (ca. 1.0×10^{13} cm^{-2} measured by SPR) of the *same* P15 sequence is used in both initial probe surfaces (P15 and P15–T5–SH in Figure S3). Compared to T15–SH probes in Figure 2, the yield for P15–T5–SH in Figure S3 is lower, most likely because the P15–T5–SH strands immobilized at ca. 30–40% lower density produce fewer upright end-tethered probes (Refs 8, 21, 22).

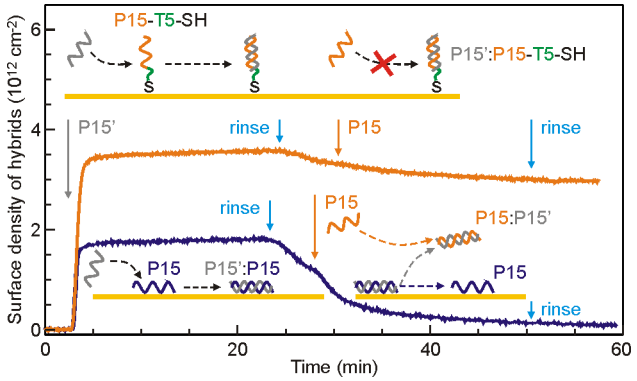

Figure S3. Different conformations of double-stranded P15:P15′ hybrids subjected to stability challenges by invasive hybridization. Diagrams depict idealized representations of each target-probe pair (orange = P15, gray = P15′, dark blue = P15 probes in directly-adsorbed conformation) through two hybridization attempts/challenges. The line colors of the data plots correspond to the respective probes: orange for end-tethered P15–T5–SH and dark blue for directly-adsorbed P15. In each experiment, the SPR sensor was sequentially exposed to: P15′ target (vertical gray arrow at ca. 3 min); blank 1 M NaCl-TE buffer (cyan arrows at ca. 23–25 min); P15 target (orange arrows at ca. 28–30 min); and the final rinse in blank buffer (cyan arrows after ca. 50 min). Hybridization conditions were the same as those in Figure S2.

When exposed to the complementary P15′ targets (vertical gray arrow at ca. 3 min in Figure S3), the end-tethered P15–T5–SH probes (orange in Figure S3) show higher hybridization activity compared to that of the directly-adsorbed P15 probes (dark blue in Figure S3). When a competitive solution of P15 targets is introduced (orange arrows at ca. 28–30 min in Figure S3), the end-tethered P15′:P15–T5–SH hybrids are barely affected, while the directly-adsorbed P15′:P15 hybrids are nearly completely disrupted (dark blue line after ca. 50 min in Figure S3).

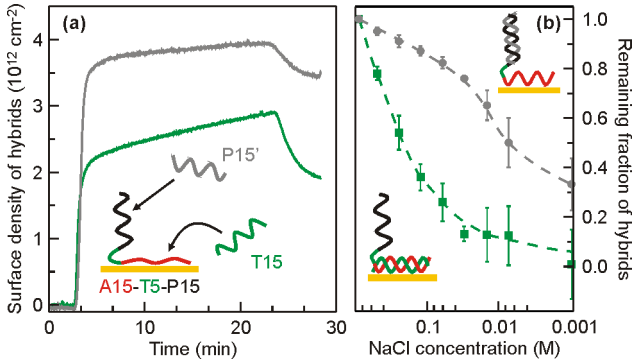

Figure S4. Formation and stability of hybrids formed with probes containing P15 and A15 sequences. Diagrams depict idealized representations of L-shape probes and their hybrids (red = adenine, green = thymine, black = P15 probe, grey = P15' target) before (a) and after (b) hybridization. The line and symbol colors in the data plots correspond to the color-coding of the respective targets: P15' (gray) or T15 (green); e.g., in (a), the green curve corresponds to A15–T5–P15+T15. Surface density of A15–T5–P15 probes was ca. 1.3×10^{13} cm^{-2}. Experimental conditions, P15 and P15' sequences were the same as in Figure S2. Error bars in (b) represent variation among replicate samples.

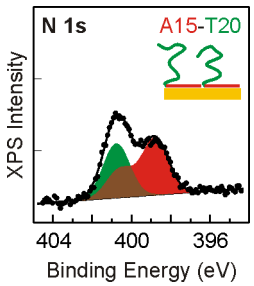

Figure S5. XPS data in N 1s region for A15–T20 model probes immobilized on gold. Immobilization was performed for 20 h from a 4 μM DNA solution in 1 M $CaCl_2$-TE buffer at 35 °C. The characteristic N 1s "singlet" and "doublet" envelopes for thymine and adenine are shaded in green and red, respectively. Each adenine and thymine nucleobase contains 5 and 2 nitrogen atoms, respectively, resulting in a proportionately stronger adenine signal. The surface density of A15–T20 probes calculated from XPS data for this sample is $1.45\pm0.10\times10^{13}$ cm^{-2}.

Single-Stranded A:T Hybrids: Fluorescence Microscopy. We use fluorescently labeled A15–T30* (* denotes TAMRA label) to take advantage of distance-dependent quenching for fluorescent molecules placed in proximity to a gold surface (Refs 13, 31, 32). Specifically for A15–T30*, such fluorescence measurements allow us to track the proximity of the TAMRA-labeled 3′ terminal to the gold surface. The longer T30 block, rather than T20 in Figure 1c, provides sufficient extension away from the gold surface for fluorescence enhancement in the putative L-shape conformation (Refs 31, 32).

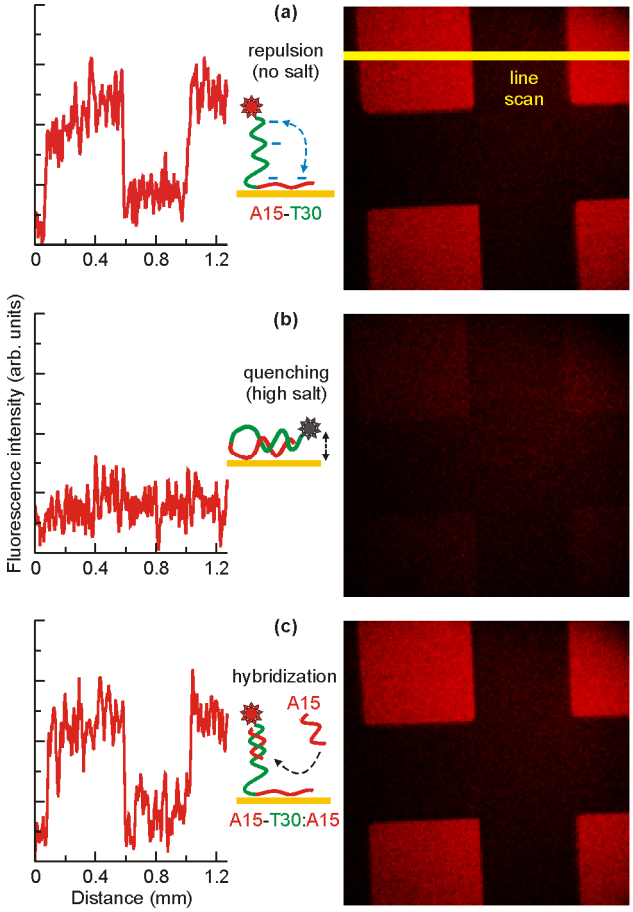

Figure S6. Conformational changes for fluorescently-labeled A15–T30* probes monitored by laser scanning confocal microscopy. Photopatterned surfaces contain 500×500 μm^2 square regions of model A15–T30* probes immobilized on clean gold surrounded by the background of gold backfilled with PEG–SH. Fluorescence images and representative line scans are shown for samples in contact with deionized water (a), 1 M NaCl-TE buffer (b), and 4 μM solution of A15 target in 1 M NaCl-TE (c). Diagrams depict idealized representations of model A15–T30* probes under the respective solution conditions (red lines = adenine, green lines = thymine); red and dark gray star-shaped polygons represent the fluorescent and quenched states of the TAMRA label, respectively; cyan "-" signs and arrow in (a) indicate electrostatic repulsion between the two sections of A15–T30*.

Figure S6 shows fluorescence images obtained from gold surfaces functionalized with directly-adsorbed A15–T30* hairpins and then placed in contact with three different solutions. Visual contrast was achieved by patterning 500×500 μm^2 square regions of fluorescent A15–T30* in a background of non-fluorescent self-assembled monolayer (SAM) of PEG–SH (Ref 15). In 1 M NaCl-TE buffer, no fluorescence is observed from the A15–T30* regions, relative to the surrounding PEG–SH regions (Figure S6b). The faint background is attributed to incomplete filtering of the excitation source and was observed in control experiments using uniform SAMs of PEG–SH on gold.

When the NaCl-TE buffer is replaced with deionized water, the fluorescence signal from the A15–T30* regions of the surface increases significantly (Figure S6a). The fluorescence enhancement and quenching is reversible over several cycles of switching between deionized water and 1 M NaCl-TE. In control experiments, fluorescence signal from TAMRA solutions changed by <20% as a function of their ionic strength and pH (Figure S7).

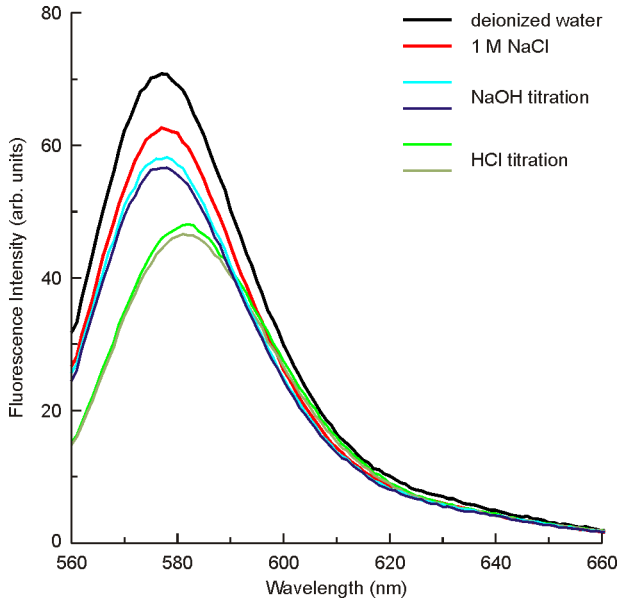

Figure S7. Variation of TAMRA fluorescence intensity with solution conditions. Changes in ionic strength or solution pH resulted in <20% variation of the TAMRA fluorescence relative to the reference intensity in 1 M NaCl.

Under the high-salt conditions of the 1 M NaCl-TE buffer, enhancement of the fluorescence signal from the A15–T30* regions is observed upon addition of A15 target (Figure S6c). This enhancement of the fluorescence signal is quantitatively similar to that observed in deionized water (cf. Figures S6a) and is also reversible. When the hybridized surface is rinsed with a denaturing 0.1 M NaOH solution and subsequently placed in 1 M NaCl-TE, the A15–T30* regions darken to the levels of Figure S6b.

Single-Stranded A:T Hybrids: NEXAFS. For label-free evaluation of hybrids formed with A*n*–T*m* probes, we used NEXAFS to characterize hybrids formed with A5–T15 probes. The short A5 block provides stable attachment for A5–T*m* probes on gold (Refs 11, 15) and reduces ambiguity of the spectral features at the nitrogen K-edge: (dA) spectral contribution is minimized before hybridization and maximized for putative A5–T15:A15 hybrids.

As previously demonstrated for model DNA films on gold (Refs 13, 22, 28, 33), NEXAFS features at the K-edge of nitrogen provide useful information about the orientation and ordering of surface-immobilized DNA molecules. NEXAFS takes advantage of linearly-polarized synchrotron x-rays to measure the variation of NEXAFS intensity as a function of the x-ray incident angle with respect to the surface (and the molecular orbitals in any film on that surface). NEXAFS selection rules (Ref 34) dictate that spectra acquired at the "magic" angle of incidence (55°) are insensitive to molecular orientation and thus characteristic of the chemical identity of samples (Figure S8a). In spectra acquired at normal (90°) and grazing (20°) angles, the contributions from π* orbitals oriented parallel and normal to the surface, respectively, are enhanced. In DNA, N π* orbitals are exclusively contained in nucleobases and are normal to the aromatic rings (Ref 22). The N π* signal is, therefore, enhanced at grazing incidence for roughly upright DNA strands; conversely, the signal is enhanced at normal incidence for directly-adsorbed (in-plane oriented) DNA strands. Plotting the difference between the spectra acquired at 20° and 90° angles of incidence conveniently visualizes the NEXAFS linear dichroism for DNA, whereby positive features indicate DNA molecules extended away from the surface (Figure S8b).

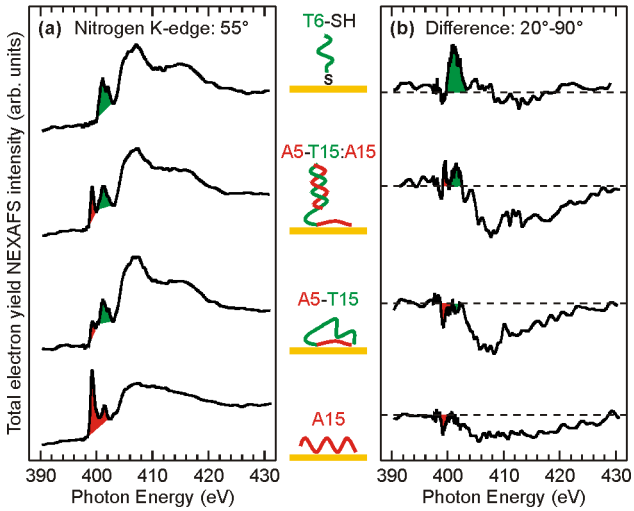

Figure S8. Nitrogen K-edge NEXAFS spectral signatures and molecular conformations in model DNA films on gold. Panels show spectra acquired with incident x-rays at 55° (a) and the difference between spectra acquired with incident x-rays at 20° and 90° (b). The spectra and diagrams in the central two rows are for a film of model A5–T15 probes (as-deposited from 3 μM solution in $CaCl_2$-TE buffer) and for a film, denoted A5–T15:A15, of the A5–T15 probes after hybridization in 3 μM solution of A15 targets in NaCl-TE buffer. Spectra for T6–SH and A15 films deposited from 3 μM solutions in $CaCl_2$-TE are shown as references for the resonance lineshapes characteristic of the respective homo-oligonucleotides (a) and the characteristic polarities of linear dichroism for upright (T6–SH) and in-plane (A15) orientations of DNA strands (b). The most pronounced features characteristic of A and T nucleobases are indicated by red and green shading, respectively. Spectra are offset for clarity, zero lines in the difference spectra are indicated by horizontal dashed lines in (b). After deposition, A15, T6–SH, and A5–T15 samples were rinsed in deionized water for ca. 1 min, while A5–T15:A15 sample was only briefly dipped into deionized water to minimize destabilization of A:T hybrids similar to that in Figure 1d.

The nitrogen K-edge NEXAFS spectra are presented in Figure S8 for four model DNA films: A5–T15 probes before and after hybridization with A15 targets, and T6–SH and A15 references. The nitrogen K-edge spectra in Figure S8a have the overall shapes typical for NEXAFS spectra of DNA films (Refs 13, 22, 28, 33), in particular, all the spectra exhibit π* resonances in the pre-edge region. The distinct lineshapes and positions of the characteristic π* resonances for adenine and thymine (shaded red and green in Figure S8, respectively) are clearly observed in the reference spectra of A15 and T6–SH and are consistent with spectra reported in the literature for similar DNA films (Refs 22, 28, 33, 35). In contrast to a complete overlap of (dA) and (dT) features in XPS N 1s data (cf. Figure S5), the separation of the most intense components of π* resonances for (dA) and (dT) allows for a qualitative assignment of the main features in the spectra of A5–T15:A15 and A5–T15 (indicated by shading in Figure S8).

A change from negative to positive dichroism is observed between spectra of A5–T15 and A5–T15:A15 in Figure S8b, as would be expected if the initial in-plane orientation of the T15 block changes to one extended away from the surface upon hybridization with an A15 target (which also is extended away from the surface as part of the same hybrid). We note that the negative dichroism observed for the A5 block of A5–T15 is consistent with the presumed in-plane orientation of the A5 attachment block, whereas after hybridization with the longer A15 targets, the (dA) component of the spectra is significantly increased and presumably dominated by the signal from the

hybrids. In agreement with the inferences from Figures 1 and 2 and from previous studies (Refs 8, 11, 20, 22, 28), dichroism signal is negative for A15 and positive for T6–SH controls, indicating in-plane and upright orientations of the respective DNA strands.

Observing the expected change in both composition (Figure S8a) and orientation (Figure S8b) between the spectra for A5–T15 and A5–T15:A15 samples is particularly significant, because the rinsing and drying procedures required before *ex situ* NEXAFS measurements can potentially interfere with the conformation and stability of any hybrids formed in solution. At least two factors likely contributed to preserving the A5–T15:A15 hybrids during an intentionally brief dip-rinse applied to the sample after hybridization. First, the data in Figures 1–2 indicate that all the end-tethered variants of A15:T15 hybrids significantly denature only after more than a few seconds (e.g., 4 min for each step in Figures 1b and 1d) in low ionic strength solutions. Second, the enhanced fluorescence in Figure S6c indicates a strong electrostatic repulsion between even partial A:T hybrids and the attachment A*n* blocks of A*n*–T*m* probes; a similar repulsion can be expected to support the roughly upright orientation of the hybrids that we observe for A5–T15:A15 sample in Figure S8b.

Single-Stranded P15′:P15 Hybrids. To examine the trends in relative stabilities of single-stranded P15′:P15 hybrids in solution and when immobilized on gold, we compare responses of thiolated P15′–T5–P15–SH hairpins (Figure S9a) and end-tethered P15–T5–SH probes (Figure S9b) to several targets that can form complete or partial hybrids with both probes.

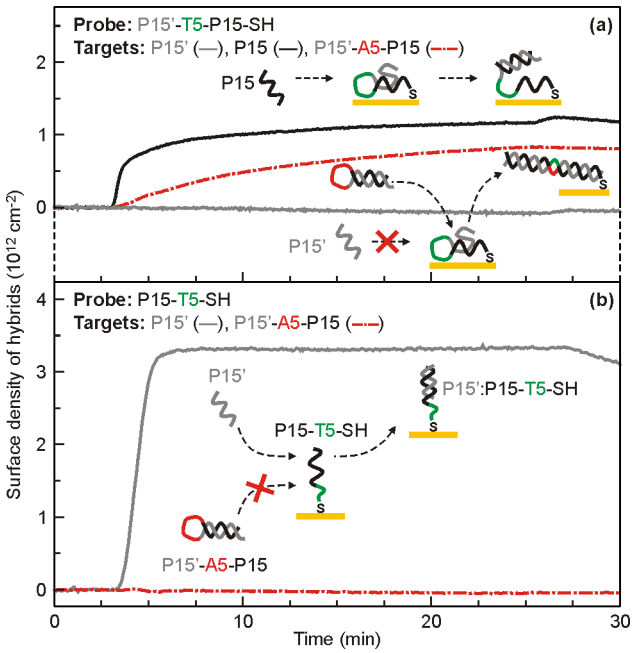

Figure S9. Asymmetric hybridization behavior of P15′–T5–P15–SH and P15–T5–SH probes exposed to full and partial complements in different conformations. SPR sensors functionalized with P15′–T5–P15–SH probes (a) were exposed to 4 μM solutions in NaCl-TE of three different targets: P15′ and P15 partial complements and P15′–A5–P15 full complement. For comparison, the simpler end-tethered P15–T5–SH probes (b) were exposed to P15′ and P15′–A5–P15 targets. Diagrams depict idealized representations of each target-probe pair (black = P15, gray = P15′, green = T15, red = A5) before and after hybridization. The line colors of the data plots correspond to the respective targets: black for P15, gray for P15′, and red dash-dot line for P15′–A5–P15.

We hypothesize that the thiol ligand on the P15 terminus of the P15′–T5–P15–SH hairpin forces the P15 block to interact with gold by proximity, making the P15–SH section analogous to the A15 "attachment block" in Figures 1c, S4–S6, and S8. Indeed, when exposed to the P15′ targets, the P15 blocks of the immobilized hairpins do not produce a detectable hybridization signal (gray line in Figure S9a). In contrast, the P15 targets can hybridize with P15′ blocks of the immobilized hairpins (black line in Figure S9a), albeit with a yield lower than that of A15–T20:A15 hybrids in Figure 1c.

The P15′:P15 hybrids enable us to expand the repertoire of probes and targets in competitive hybridization measurements: in addition to challenging hairpin probes with single-stranded targets (Figures 1, 3, S6), we also can challenge single-stranded probes (both folded and unfolded) with *hairpin targets* (red dash-dot lines in Figure S9). Figure S9b illustrates this approach for end-tethered single-stranded P15–T5–SH probes, which, of course, readily hybridize with P15′ targets (gray line in Figure S9b, cf. Figures S2 and S3). In contrast, P15′–A5–P15 *hairpin targets* that include the same P15′ target sequence do not produce any hybrids with the P15–T5–SH probes (red dash-dot line in Figure S9b), i.e., a hypothetical reaction that involves opening a solution single-stranded P15′:P15 hairpin hybrid to form an end-tethered *partial* double-stranded P15–A5–P15′: P15–T5–SH hybrid does not proceed. End-tethered *full* hybrids between P15′–A5–P15 targets and P15′–T5–P15–SH probes, however, are energetically favorable, as this type of hybridization proceeds in Figure S9a (red dash-dot line) despite requiring two hairpins to denature in the process.